Energetics of Coiled Coil Folding: The Nature of the Transition States[†]

Hans Rudolf Bosshard,* Eberhard Dürr,[‡] Thomas Hitz,[§] and Ilian Jelesarov

Biochemisches Institut der Universität Zürich, Winterthurerstrasse 190, CH-8057 Zürich, Switzerland

Received September 13, 2000; Revised Manuscript Received December 14, 2000

ABSTRACT: Coiled coils are simple models for studying the association of two polypeptide chains to form a folded protein. Previous work has shown that the folding of a coiled coil can be described by a two-state transition between two unfolded monomeric peptide chains and a folded coiled coil dimer. Here we report the thermodynamic activation parameters for the folding and unfolding of two unrelated coiled coils: C62GCN4 and A_2. C62GCN4 corresponds to the 62 C-terminal residues of yeast transcription factor GCN4. The peptide forms a dimeric coiled coil through its 33 C-terminal residues. A_2 is a designed 30-residue dimeric coiled coil whose folding is induced by low pH [Dürr, E., Jelesarov, I., and Bosshard, H. R. (1999) *Biochemistry 38*, 870−880]. Folding and unfolding were assessed under identical native buffer conditions so that the microscopic reversibility applied and the transition state was the same for folding and unfolding. The time course of folding was followed from the self-quenching of a C-terminal fluorescent label (Texas Red). The overall folding of both peptides is enthalpy-driven and opposed by a loss of entropy. The main energetic changes occur after the system has passed the transition state. In the folding of C62GCN4, only 10−20% of the heat capacity change is attained between the monomeric state and the dimeric transition state. For coiled coil A_2, the fractional heat capacity change preceding the transition state is 30−40%. The results indicate that the activated states of folding of coiled coils are not well structured and differ considerably from the folded coiled coil conformation. These findings are in agreement with a rate-limiting transition state in which the coiled coil helices and the hydrophobic coiled coil interface are poorly developed.

Elucidating the mechanism of protein folding is a major challenge of biochemistry. Folding transitions of many proteins have been studied and have led to insights into conformational properties of partially folded intermediates and rate-limiting transition states. A coherent picture of this phenomenal process of nature is now slowly emerging (recent reviews in refs *1*−*4*). Most studies on protein folding have dealt with monomeric proteins. There may be complications to the folding reaction if a protein is composed of two or more subunits and if the subunits in isolation do not fold to a thermodynamically stable state. In this case, the folding of the individual subunits and their association to form the multimeric native state are coupled reactions.

A very simple model for coupled folding and association is the assembly of a coiled coil. It is a helical dimerization motif found in a wide variety of proteins (*5*−*7*). The motif consists of two amphipathic α-helical peptides wound around each other at an angle of ∼20°. Because hydrophobic side chains extend along one face of each helix, the coiled coil is stabilized by hydrophobic packing along the dimer interface, and each helix alone is thermodynamically unstable in an aqueous environment. The amphipathic structure originates from a seven-residue sequence motif, $(abcdefg)_n$, repeating every two α-helical turns and containing mostly hydrophobic residues at the *a* and *d* positions. Short coiled coils composed of four or five heptads are found in transcription factors and are called leucine zippers because leucines are frequent in *d* positions and interdigitate at the dimer interface as in a zipper (*7*−*10*).

Many natural and designed coiled coils fold by a simple two-state transition between monomer M and dimer D with no indication of a stable intermediate state. The rate of folding may even approach the diffusion-limited rate of encounter of two unfolded peptide chains (*11*, *12*). Hence, folding and association are indeed strongly coupled. It has been proposed that coiled coils form by a hydrophobic collapse mechanism in which two unfolded monomers associate through a rate-limiting transition state. Much of the hydrophobic surface is thought to be buried in the transition state in which helical structure is not yet well developed and forms subsequently in a very rapid, energetically "downhill" reaction (*13*). Very rapid folding does, however, not exclude the possibility that helical structure is formed *before* the rate-limiting transition state. For example, in a diffusion−collision model (*14*), prefolded helical or partly helical monomers would associate productively to form the coiled coil. Indeed, there is evidence for a "trigger sequence" proposed to adopt a helical conformation in the monomer and to be indispensable for successful association and folding (*15*, *16*). A small helix-forming propensity calculated for the GCN4-p1 leucine zipper monomer has been taken to indicate folding through association of partly helical monomeric peptides (*17*).

[†] This work was supported in part by the Swiss National Science Foundation (Grant 31.55308.98) and by the European Commission (Grant BBW 970592).

[‡] Present address: Sidney Kimmel Cancer Center, 10835 Altman Row, San Diego, CA 92121.

[§] Present address: Institut für Polymere, CAB E 35, ETH-Zentrum, Universitätsstrasse 6, CH-8092 Zürich, Switzerland.

10.1021/bi002161l CCC: $20.00
Published on Web 03/01/2001

To better understand how coiled coils fold, we need more information about the rate-limiting formation of the transition state of folding. One well-tested way to deduce the structure of the transition state of folding is Φ analysis, which infers the extent of inter-residue contact in the transition state from a combination of single-residue mutations and rate measurements (*18*−*20*). A Φ value of 1 indicates that the site which is mutated is structured as much in the transition state as in the native state. A Φ value of 0 indicates that the site of mutation is not yet structured in the transition state. Ala → Gly substitutions lower the helix-forming propensity and should produce Φ values close to 0 if the site of the Ala → Gly mutation is not yet helical in the transition state of coiled coil folding. In one study of the GCN4-p1 leucine zipper, Ala → Gly substitutions had indeed only a modest effect on the folding rate and Φ values were small, from which it was inferred that not much helix is present before the two peptides collide in a productive way to form the coiled coil (*13*, *21*). However, the conclusion has been challenged recently by another mutational study which concluded that helix formation in at least a portion of the GCN4-p1 sequence is required to form the dimeric transition state (*17*, *22*). At present, the degree of helix formation and surface burial in the rate-limiting step of coiled coil folding is under debate (*13*, *17*, *21*, *22*). This has prompted us to study the temperature dependence of folding and unfolding of two short coiled coils so that we can calculate the activation parameters of folding by applying classical transition state theory. The extent of surface burial in the transition state can then be estimated from the fractional change of the heat capacity, $\Delta C_p^{\ddagger}$ (*23*, *24*).

Although classical transition state theory has been developed for simple chemical reactions of small molecules, it can be applied to a two-state protein folding system where only the unfolded and the folded states are noticeably populated at any time. Also, one has to consider that the transition state of protein folding is not unique but composed of an ensemble of structurally more or less related states (*4*, *25*−*27*). With these limitations in mind, we have determined the activation parameters $\Delta G^{\ddagger}$, $\Delta H^{\ddagger}$, $\Delta S^{\ddagger}$, and $\Delta C_p^{\ddagger}$ for the folding and unfolding of the coiled coils C62GCN4 and A_2. C62GCN4 corresponds to the 62 C-terminal residues of yeast transcription factor GCN4 (*28*). Dimer A_2 is a designed coiled coil formed from two 30-residue acidic peptides whose formation is induced by low pH (*12*). The two unrelated peptides were selected in the hope of detecting energetic features that are common to the folding of coiled coils. The results point to relatively nonstructured transition states in which considerably less molecular surface is buried than in the final coiled coil.

MATERIALS AND METHODS

Materials

Peptides. Peptides C62GCN4 and C62GCN4C were expressed in *Escherichia coli* as described previously (*29*, *30*). To obtain C62GCN4C^{TR}, the Texas Red fluorescent label was introduced by reacting 0.5 μmol of C62GCN4C in 6 mL of reaction buffer [50 mM sodium phosphate, 6 M GdmCl,[1] and 10% glycerol (pH 7.6)] with 4 μmol of Texas Red C5-bromoacetamide (compound T-6009 from Molecular Probes, Eugene, OR) in 23 mL of reaction buffer. The reaction was conducted for 4 h at 20 °C in the dark and in an argon atmosphere to prevent oxidation of Cys. The reaction was stopped by addition of excess dithiothreitol. The product was desalted by dialysis and purified by HPLC on a reversed phase column (Nucleosil 300-5C8), which was eluted with a binary gradient of acetonitrile and water containing 0.1% trifluoroacetic acid. Peptide A and the labeled derivative Flu-A were synthesized as described previously (*12*). The homogeneity of the peptides was checked by mass spectrometry. Peptide concentrations were determined from UV absorption measurements in 6 M GdmCl ($\epsilon_{275.3} = 1450\ M^{-1}\ cm^{-1}$) (*31*). The concentration of C62GCN4C^{TR} was calculated from visible absorption measurements ($\epsilon_{583} = 113\,000\ M^{-1}\ cm^{-1}$) (*32*). Concentration is always expressed as total peptide concentration ($[C_0]$); for example, 1 μM peptide corresponds to 0.5 μM dimeric coiled coil.

Buffers. Buffer A was 50 mM sodium phosphate, 10 mM $MgCl_2$, and 10 mM NaCl (pH 7.4). Buffer B was buffer A containing in addition 4 M GdmCl. Buffer C was phosphoric, citric, and boric acid (7.5 mM each) adjusted to the desired pH with KOH or HCl and adjusted to an ionic strength of 0.1 M with KCl.

Methods

Rapid Mixing Experiments. Folding kinetics were studied with an SF-61 stopped-flow spectrofluorimeter (High Tech Scientific Ltd., Salisbury, U.K.). The reaction cell of this instrument is temperature-controlled to ±0.3 °C. The dead time of the instrument is 1−2 ms. Excitation of Flu-A was at 485 nm, and emission was measured at >530 nm. Excitation of C62GCN4C^{TR} was at 583 nm, and emission was measured at >590 nm. Folding of C62GCN4C^{TR} was initiated by rapid dilution of the peptide dissolved in buffer B, with 20 volumes of buffer A; the final peptide concentration after dilution was 0.6 μM. Folding of Flu-A was initiated by rapid dilution of the peptide dissolved in buffer C at pH 12, with 20 volumes of buffer C at pH 4.4 or 4.9; the final peptide concentration after dilution was 0.6 μM. Samples were collected after each rapid mixing reaction to control the temperature-corrected pH value, which was constant within ±0.1 pH unit. Experiments with C62GCN4C^{TR} were performed at 13 different temperatures from 5 to 30 °C. Experiments with Flu-A were performed at 19 different temperatures from 5 to 50 °C. The results of 10−20 syringe firings were averaged at each temperature. Triplicate measurements were carried out with peptide Flu-A.

Data Analysis of Rapid Mixing Experiments. Traces were analyzed for the two-state transition

$$2M \underset{k_{off}}{\overset{k_{on}}{\rightleftharpoons}} D \qquad (1)$$

where k_{on} and k_{off} are the rate constants of association (second-order rate constant) and dissociation (first-order rate constant), respectively. The fluorescence change during

[1] Abbreviations: CD, circular dichroism; DSC, differential scanning calorimetry; Flu, fluorescein; GCN4, general control of amino acid synthesis non-derepressible mutant 4; GdmCl, guanidinium chloride; HPLC, high-performance liquid chromatography; TR, Texas Red; M, ts, and D, monomeric peptide, dimeric transition state, and dimeric folded coiled coil, respectively.

Table 1: Activation Parameters of the Folding of the GCN4 Leucine Zipper at pH 7.4 and 20 °C[a]

	2M → ts	ts → D	2M → D[b]	global fit[c]
$\Delta C_p^{\ddagger}$ (kJ mol^{-1} K^{-1})	−0.38 ± 0.35	−2.33 ± 0.56	−2.71 ± 0.91	−2.80 ± 0.12 ca. −3.00[d]
$T\Delta S^{\ddagger}$ (kJ mol^{-1})	7.9 ± 2.8	−60 ± 1	−52.1 ± 3.8	−55.8[e]
$\Delta H^{\ddagger}$ (kJ mol^{-1})	20.7 ± 2.8	−116 ± 5	−95.3 ± 7.8	−99 [f]
$\Delta G^{\ddagger}$ (kJ mol^{-1})	12.8 ± 0.1	−56 ± 1	−43.2 ± 1.1	−43.2
T_g (K)[g]			375 ± 1	373 ± 1

[a] Experimental errors refer to the fitting procedure. [b] Sum of activation parameters for 2M → ts and ts → D. [c] From the global fit to kinetic and equilibrium thermodynamic data shown in Figure 3. [d] Estimated by extrapolation of the heat capacity trace of the unfolded protein to 20 °C (Figure 2B). [e] From $T\Delta S = \Delta H - \Delta G$. [f] From $\Delta H = \Delta H_m + \Delta C_p(T - T_m)$. [g] T where $\Delta G = 0$ and $\Delta H = T_g\Delta S$.

Table 2: Thermodynamic Parameters from Thermal Unfolding of the Leucine Zipper C62GCN4 Observed by CD and DSC (Units Are Kilojoules per Mole and Kelvin, Respectively[a])

	CD			DSC			
[C_0] (μM)	T_m	ΔH_m	ΔG_m[b]	T_m	ΔH_m^{vH}[c]	ΔH_m^{cal}[d]	ΔG_m[b]
50	334.6	305	27.6				
154	338.1	330.7	24.7	340.8[e]		293	24.9
154				339.2[f]	280		24.8
208	341	282	24.1	342.4[e]		272	24.1
208				340.5[f]	284		24.0
480	344.6	286	21.9	346.3[e]		305	22.0
480				344.7[f]	303		21.9

[a] Errors in T_m are approximately ±0.25 K and in ΔH_m approximately ±10%. [b] ΔG_m calculated from the equation $\Delta G_m = -RT_m \ln[C_0]$. [c] Enthalpy change calculated assuming the heat absorption peak (Figure 2B) represents a two-state transition (see ref *12* for details). [d] Excess enthalpy calculated by integration of the heat absorption peak (Figure 2B). $\Delta H_m^{vH} \sim \Delta H_m^{cal}$ for a two-state transition (see ref *12* for details). [e] Temperature at the maximum of the heat capacity trace. [f] Temperature where the transition is half-completed.

refolding (fluorescence decrease) is described by

$$F(t) = \Delta F_{max}\left(\frac{[M]}{[C_0]}\right) + F_\infty \qquad (2)$$

where $F(t)$ is the fluorescence at time t, ΔF_{max} the maximum fluorescence change, F_∞ the fluorescence at infinite time, and $[C_0]$ the total peptide concentration. The rate of folding or unfolding is described by

$$-{}^1/_2\left(\frac{d[M]}{dt}\right) = k_{on}[M]^2 - k_{off}\left(\frac{[C_0] - [M]}{2}\right) \qquad (3)$$

To obtain k_{on} and k_{off}, the kinetic traces were analyzed by nonlinear curve fitting (programs Origin 4.1, MicroCal Software Inc., or SigmaPlot 5.0, Jandel Scientific Inc.) with the help of eq 2 and with [M] defined by the integral of eq 3 (*33*). Results were not affected by the small change in intrinsic emission of the fluorescent label with pH since the change occurred within the dead time of mixing. Using this approach, both rate constants could be obtained under the same reaction conditions by analyzing single traces since refolding and unfolding both contributed to the observed traces under the conditions of the experiment (*11*, *12*, *33*). Fitting errors were 2−5% for k_{on} and k_{off} except in the case of k_{off} for $(Flu\text{-}A)_2$, for which the error was large. Therefore, k_{off} for this peptide was also calculated from the relation $K_a = k_{on}/k_{off}$ using values of K_a determined previously (values from Figure 10 of ref *12*). The calculated k_{off} values were used to obtain the activation parameters of Table 3 and the data shown in Figure 4.

Reversible Equilibrium Unfolding and Folding Followed by CD Spectroscopy and by DSC. Experiments were performed and data analyzed as described previously (*12*).

Transition State Analysis. There is very good evidence that the coiled coil domains of GCN4 (*13*, *21*, *22*, *34*−*36*) and of other leucine zippers (*11*, *37*, *38*) fold according to a two-state model, with a negligible population of intermediates (eq 1). For peptides A and Flu-A, we had shown before that folding is strictly two-state over a wide range of pHs and temperatures (*12*, *38*). Two-state folding is a prerequisite for applying conventional transition state theory to analyze rate data. In this theory, the state with the highest energy, also called the activated state, is treated as a defined state in equilibrium with reactants and products through a quasi-equilibrium constant $K^{\ddagger}$ (*39*). The rate of product formation k depends on the free activation energy $\Delta G^{\ddagger} = -RT \ln K^{\ddagger}$ according to the Eyring equation:

$$k = \kappa k_0 \exp(-\Delta G^{\ddagger}/RT) \qquad (4)$$

κ is a dimensionless factor and was set at 1 in the present analysis (see the Discussion). k_0 is a temperature-dependent factor whose magnitude influences the absolute values of $\Delta S^{\ddagger}$ and, hence, of $\Delta G^{\ddagger}$. k_0 does not affect $\Delta H^{\ddagger}$ and $\Delta C_p^{\ddagger}$ as long as the temperature dependence of k_0 is small and $\Delta C_p^{\ddagger}$ is temperature-independent (*4*). In classical transition state theory, $k_0 = k_B T/h = 6 \times 10^{12}$ s^{-1} at 20 °C (k_B is the Boltzmann constant and h Planck's constant). In the present study, we used a k_0 of 10^9 s^{-1} at 20 °C for reasons explained in the Discussion.

Equation 4 can be decomposed according to the relationship $\Delta G^{\ddagger}(T) = \Delta H^{\ddagger}(T) - T\Delta S^{\ddagger}(T)$. If it is assumed that the heat capacity change $\Delta C_p^{\ddagger}$, which governs the dependence of $\Delta H^{\ddagger}$ and $\Delta S^{\ddagger}$ on T, is itself temperature-independent in the narrow temperature interval of the experiment, one obtains (*25*)

$$\ln(k/k_0) = A + B(T_R/T) + C \ln(T_R/T) \qquad (5)$$

$$A = -(\Delta C_p^{\ddagger} - \Delta S_R^{\ddagger})/R = -[(\Delta C_p^{\ddagger} - (\Delta H_R^{\ddagger} - \Delta G_R^{\ddagger})/T_R]/R$$

$$B = (\Delta C_p^{\ddagger} - \Delta S_R^{\ddagger} - \Delta G_R^{\ddagger}/T_R)/R = \Delta C_p^{\ddagger}/R - [(\Delta H_R^{\ddagger} - \Delta G_R^{\ddagger})/T_R]/R - \Delta G_R^{\ddagger}/RT_R$$

$$C = -\Delta C_p^{\ddagger}/R$$

The subscript R indicates a reference temperature, which we chose to be 293.15 K (20 °C). The rate constant k of eq 5 refers to either k_{on} or k_{off}. In Figures 1 and 4, the measured

Table 3: Activation Parameters at 20 °C of the Folding of Coiled Coil A_2 at pH 4.4 and 4.9, Respectively[a]

	pH	2M → ts	ts → D	2M → D[b]	global fit[c]
$\Delta C_p^{\ddagger}$ (kJ mol^{-1} K^{-1})	4.4	−0.69 ± 0.15	−1.18 ± 0.15	−1.87 ± 0.30	−1.99 ± 0.07
	4.9	−0.73 ± 0.67	−1.08 ± 0.68	−1.81 ± 1.35	
$T\Delta S^{\ddagger}$ (kJ mol^{-1})	4.4	4.0 ± 0.2	−105 ± 1	−101 ± 1	−97.1[d]
	4.9	−25.4 ± 0.4	−84 ± 4	−110 ± 4	
$\Delta H^{\ddagger}$ (kJ mol^{-1})	4.4	13.2 ± 1.3	−162 ± 1	−149 ± 2	−146[e]
	4.9	−14.4 ± 4.0	−135 ± 3	−149 ± 7	
$\Delta G^{\ddagger}$ (kJ mol^{-1})	4.4	9.2 ± 0.1	−57.2 ± 0.1	−48 ± 0.2	−48.8
	4.9	11.0 ± 0.2	−51.4 ± 0.2	−40.4 ± 0.4	
T_g (K)[f]	4.4			376 ± 2	375 ± 2
	4.9			366 ± 1	363 ± 1

[a] Experimental errors refer to the fitting procedure. [b] Sum of activation parameters for 2M → ts and ts → D. [c] From the global fit to kinetic data (Figure 4) and equilibrium thermodynamic data (*12*) at pH 4.4. [d] From $T\Delta S = \Delta H - \Delta G$. [e] From $\Delta H = \Delta H_m + \Delta C_p(T - T_m)$. [f] T where $\Delta G = 0$ and $\Delta H = T_g\Delta S$.

rate constants are plotted according to eq 5 as $\ln(k/k_0)$ versus T, where k_0 (s^{-1}) = 3.4 × 10^6 × T (from 10^9 s^{-1}/293 K = 3.4 × 10^6 s^{-1} K^{-1}).

The activation parameters $\Delta J^{\ddagger}$ ($J = G$, H, S, and C_p) are obtained by fitting experimental values of k_{on} and k_{off} measured over a range of temperatures. In eq 5, $\Delta J^{\ddagger}$ is defined as $\Delta J^{\ddagger}_{2M\rightarrow ts} = J^{ts} - J^{2M}$ for the folding direction 2M → ts, and as $\Delta J^{\ddagger}_{D\rightarrow ts} = J^{ts} - J^{D}$ for the unfolding direction D → ts. When the unfolded state M is taken as the reference state, the equilibrium thermodynamic parameters are $\Delta J_{2M\rightarrow D} = (J^{ts} - J^{2M}) - (J^{ts} - J^{D})$. However, we prefer to change the sign of the unfolding activation parameters and use the following definitions throughout the rest of this paper:

$$\Delta J^{\ddagger}_{2M\rightarrow ts} = J^{ts} - J^{2M} \quad (6a)$$

$$\Delta J^{\ddagger}_{ts\rightarrow D} = J^{D} - J^{ts} \quad (6b)$$

$$\Delta J_{2M\rightarrow D} = \Delta J^{\ddagger}_{2M\rightarrow ts} + \Delta J^{\ddagger}_{ts\rightarrow D} \quad (6c)$$

In this way, the overall folding reaction can be regarded as the sum of the transitions 2M → ts and ts → D. This facilitates the discussion since the equilibrium thermodynamic parameters are now the sum of the parameters from 2M to ts and from ts to D. For example, the equilibrium heat capacity change becomes the sum of the heat capacity changes accomplished before and after the transition state ($\Delta C_{p,2M\rightarrow D} = \Delta C_p^{\ddagger}{}_{2M\rightarrow ts} + \Delta C_p^{\ddagger}{}_{ts\rightarrow D}$).

The nature of the activated state can depend strongly on experimental conditions as shown, for example, for the folding of Tendamistat (*40*). However, transition state theory assumes that folding and unfolding pass through the same activated state. It is therefore important to measure the folding and unfolding rate constants under identical experimental conditions so that microscopic reversibility applies. This was achieved by calculating both rate constants from the same kinetic trace (eqs 2 and 3) instead of from rapid dilution into denaturant and out of denaturant, respectively, as is commonly done.

RESULTS

Folding of C62GCN4. The GCN4 derivative used in this study has the sequence M[220]IVPESSDPAAL*KRARN-TEAARRSRARK*LQRMKQLEDKVEELLSKNYHLENE-VARLKKLVGE[281]R. This is the C-terminal 220−281 sequence of the yeast transcriptional regulator GCN4. The N-terminal Met is from the overexpression construct (*28*, *29*). The peptide contains the basic region DNA binding domain (in italics) and the C-terminal leucine zipper domain (underlined). The basic region DNA binding domain has no stable conformation (*41*) and only folds to an α-helix when bound to the major groove of the target DNA (*28*, *41*−*43*). Thus, in the absence of DNA, only the folding of the C-terminal coiled coil of C62GCN4 is being observed in this study.

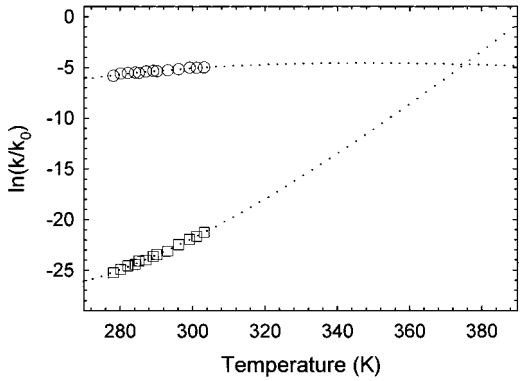

FIGURE 1: Temperature dependence of the folding rate constant (○) and the unfolding rate constant (□) for C62GCN4C^{TR}. The dotted lines are best fits according to eq 5. For the folding reaction, $k = k_{on}$[peptide] where [peptide] = 1 mol/L. For the unfolding reaction, $k = k_{off}$. See Table 1 for thermodynamic parameters obtained from the fits and the text for further details.

Peptide C62GCN4C is peptide C62GCN4 with the C-terminal extension GSGC (*30*). In C62GCN4C^{TR}, the fluorescent label TR is attached to the C-terminal cysteine through a thioether bond and provides a fluorescence tag for following the time course of folding (*44*, *45*). The charged aromatic fluorescent labels do not by themselves induce dimer formation since there is no quenching when the peptides cannot dimerize (*44*−*46*).

The kinetics of folding of C62GCN4C^{TR} were measured between 5 and 30 °C at pH 7.4. Folding was initiated by rapid dilution from 4 to 0.2 M GdmCl. Between 5 and 30 °C, the folding rate of 0.6 μM peptide increases from 3.3 to 8.4 s^{-1} and the unfolding rate from 0.01 to 0.6 s^{-1}. The results are shown in Figure 1. The change in heat capacity between the unfolded state and the transition state is small in comparison to the change from the transition state to the folded state, where $\Delta C_p^{\ddagger}{}_{2M\rightarrow ts} = -0.38 \pm 0.34$ kJ mol^{-1} K^{-1} versus $\Delta C_p^{\ddagger}{}_{ts\rightarrow D} = -2.33 \pm 0.56$ kJ mol^{-1} K^{-1} (Table 1). Despite the large fitting errors (due to the small change in

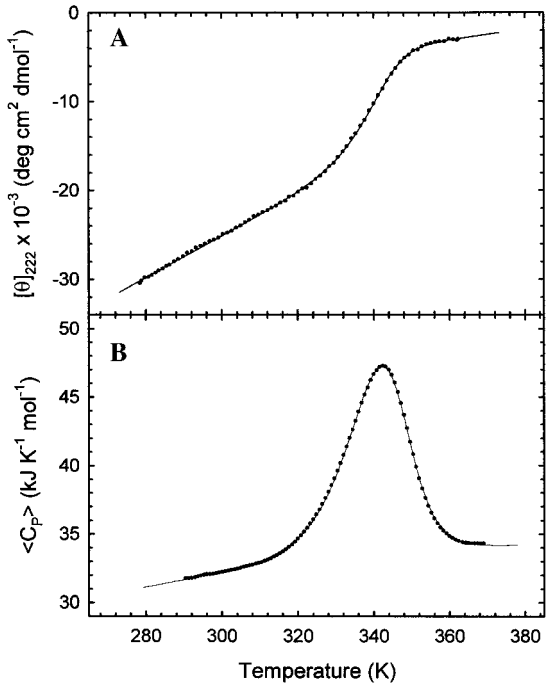

FIGURE 2: CD thermal melting curve (A) and DSC melting trace (B) for 208 μM peptide C62GCN4 in buffer A.

k_{on} with T), it is obvious that most of the change in the heat capacity takes place after the transition state. This also follows from the much stronger change of k_{off} with T (Figure 1). The absolute values of the activation enthalpy, activation entropy, and activation free energy for the transition 2M → ts are small when compared to the values for the transition ts → D. At 20 °C, formation of the activated state is favored by a small positive activation entropy change $T\Delta S^{\ddagger}_{2M\rightarrow ts}$ of 7.9 kJ mol^{-1} and opposed by a larger positive activation enthalpy change $\Delta H^{\ddagger}_{2M\rightarrow ts}$ of 20.7 kJ mol^{-1}, resulting in an overall unfavorable $\Delta G^{\ddagger}_{2M\rightarrow ts}$ of 12.8 kJ mol^{-1}. However, one has to keep in mind that $T\Delta S_{2M\rightarrow ts}$ depends on the chosen pre-exponential factor k_0 of eq 4, which we have set at 10^9 s^{-1} (see the Discussion). If the "classical" pre-exponential factor k_BT/h of 6×10^{12} s^{-1} (20 °C) is used, one obtains a $T\Delta S^{\ddagger}_{2M\rightarrow ts}$ of −25 kJ mol^{-1} and a $\Delta G^{\ddagger}_{2M\rightarrow ts}$ of 45.7 kJ mol^{-1}. Thus, the magnitude and sign of $T\Delta S^{\ddagger}$ and, hence, the absolute barrier height $\Delta G^{\ddagger}$ have to be interpreted with caution. All we can conclude from the data of Table 1 is that (i) the energetically unfavorable realization of the transition state has a positive enthalpy component and (ii) the bulk of the energetic change of the folding reaction is achieved beyond the activated state.

To further support the two-state folding model on which the transition state analysis rests and to show that the bulky C-terminal fluorescent label TR of C62GCN4C^{TR} does not affect the energetics of folding, we measured the equilibrium thermodynamic parameters for C62GCN4, which lacks the C-terminal extension with the TR label. CD spectra of C62GCN4 were recorded in the range of 5−90 °C at pH 7.4 in buffer A. The ellipticity minimum at 222 nm, which signifies α-helical structure, shows a typical reversible transition from helical to random coil (Figure 2A). The same reversible transition was also seen by DSC (Figure 2B). Thermal unfolding was >95% reversible. Equilibrium parameters obtained from the CD and DSC melting curves are summarized in Table 2. The combined kinetic and equilibrium thermodynamic data are shown in Figure 3. The experimental data were analyzed with the help of eq 7 (solid line in Figure 3).

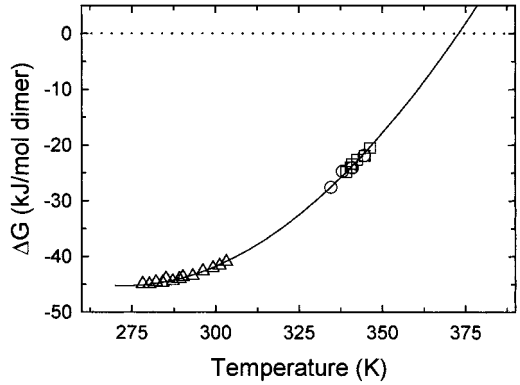

FIGURE 3: Combined kinetic and equilibrium thermodynamic data for the GCN4 leucine zipper with a global fit according to eq 7. (△) $\Delta G = -RT \ln(k_{on}/k_{off})$ from kinetic data for fluorescently labeled C62GCN4C^{TR}. (○) ΔG from thermal unfolding of C62GCN4 observed by CD (Figure 2A). (□) ΔG from thermal unfolding of C62GCN4 observed by DSC (Figure 2B). The solid line is the best fit (eq 7) for $\Delta H_m = -232.5$ kJ mol^{-1}, $\Delta C_p = -2.80$ kJ mol^{-1} K^{-1}, $T_m = 340.5$ K, and $[C_0] = 208$ μM.

$$\Delta G(T) = \Delta H_m(1 - T/T_m) + \Delta C_p[(T - T_m - T\ln(T/T_m)] - RT\ln[C_0] \quad (7)$$

The fit is good, and values of ΔC_p from the global fit and from the kinetic data alone are the same within error (Table 1). ΔC_p estimated from the DSC trace by extrapolating the heat capacity of the unfolded peptide in Figure 2B to 20 °C is approximately −3 kJ mol^{-1} K^{-1}, in agreement with ΔC_p from kinetics and global data analysis. The temperatures T_g (Table 1) at which $\Delta G = 0$ and $\Delta H = T_g\Delta S$ are very similar when extrapolated from the intersection of the dotted lines in Figure 1 and from extrapolation to $\Delta G = 0$ in Figure 3. The congruence of the kinetic and equilibrium thermodynamic data shows that the bulky TR fluorescence group used to follow the folding kinetics does not change the folding energetics.

Folding of Coiled Coil A_2. Peptide A has the sequence Ac-EYQALEKEVAQLEAEENQALEKEEVAQLEHEG-amide. The peptide folds to the homodimeric coiled coil A_2 when the pH is lowered, with a midpoint at pH 5.2 (*12*). The energetics of folding of A_2 have been studied over a broad temperature range by CD spectroscopy and DSC in a recent study (*12*). Protonation of the glutamic acid residues in the *e* and *g* positions of each heptad increases hydrophobicity (weaker dipole moment of protonated Glu) and stabilizes the coiled coil dimer (*12, 47*). To follow the time course of folding and unfolding, peptide Flu-A containing the N-terminal extension fluoresceinyl-GGG was used. Fluorescence emission is quenched in the folded coiled coil (*12, 38*). The fluorophore affects neither the equilibrium thermodynamic parameters nor the kinetics of folding (*12, 44−46*).

Folding of peptide Flu-A was assessed between 5 and 50 °C at pH 4.4 and 4.9. Folding was initiated by rapid dilution from pH 12 to 4.4 or 4.9. Between 5 and 50 °C, the folding rate of 0.6 μM peptide increases from 16 to 36 s^{-1} and the unfolding rate from 2 to ∼100 s^{-1}. The results are shown in

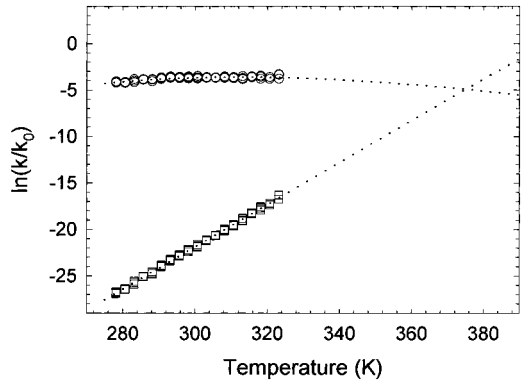

FIGURE 4: Temperature dependence of the folding rate constant (○) and the unfolding rate constant (□) for peptide Flu-A at pH 4.4. The dotted lines are best fits according to eq 5. For the folding reaction, $k = k_{on}$[peptide] where [peptide] = 1 mol/L. For the unfolding reaction, $k = k_{off}$. See Table 3 for thermodynamic parameters obtained from the fits and the text for further details.

Figure 4 and Table 3. As observed for the GCN4 leucine zipper, the difference in the heat capacity between the unfolded state and the transition state is relatively small; 30−40% of the overall heat capacity change is achieved before the activated state. Again, the absolute values of $\Delta H^{\ddagger}$, $\Delta S^{\ddagger}$, and $\Delta G^{\ddagger}$ are small for the transition 2M → ts and large for the transition ts → D. Since the folding free energy ΔG is a strong function of pH (*12*), the activation parameters differ when measured at pH 4.4 and 4.9 (Table 3). To obtain a global fit to the kinetic and equilibrium data, ΔG [$=-RT \ln(k_{on}/k_{off})$ (present data)] and ΔG values obtained from CD and DSC melting curves (Tables 1 and 2 and Figure 9 of ref *12*) were combined in the same way as shown for C62GCN4 in Figure 3. The parameters from the global fit agree with the data from kinetics alone (Table 3).

DISCUSSION

Validity of Activation Parameters. The magnitude of the pre-exponential factor k_0 of the Eyring equation (eq 4) influences the absolute values of $\Delta S^{\ddagger}$ and $\Delta G^{\ddagger}$, whereas $\Delta H^{\ddagger}$ and $\Delta C_p^{\ddagger}$ are not affected by k_0 as long as the temperature dependence of k_0 is small and $\Delta C_p^{\ddagger}$ is temperature-independent (*4*). Therefore, values of $\Delta H^{\ddagger}$ and $\Delta C_p^{\ddagger}$ obtained by applying transition state theory are more reliable than those of $\Delta S^{\ddagger}$ and $\Delta G^{\ddagger}$. In conventional transition state theory, $k_0 = k_B T/h$, $\sim 10^{12}$ s^{-1} around room temperature. This value seems inappropriate for protein folding, which involves motion of the peptide chain in solution and making and breaking many noncovalent bonds within the peptide chain and between the peptide chain and the solvent. There have been several attempts to estimate the pre-exponential factor for the folding of monomeric proteins, taking into account contributions from intrachain motion and inter- and intramolecular frictional terms (*48*, *49*; review in ref *50*). In the case of the coupled folding and association of a coiled coil, we are fortunate in that we may assume the pre-exponential factor reflects a folding reaction in which each encounter of two monomeric peptide chains is successful. In other words, k_0 may be likened to the diffusion-limited rate of encounter of two peptide chains in aqueous solution. At 20 °C, this rate is estimated to be 5×10^9 M^{-1} s^{-1} for a hydrated globular molecule with the mass of peptide A (*12*). Indeed, the maximum rate of acid-induced folding of Flu-A extrapolates to 3×10^8 M^{-1} s^{-1} (*12*). An even larger value is extrapolated for the maximum rate of folding of an electrostatically stabilized coiled coil, 9×10^9 M^{-1} s^{-1} (*11*). We choose 10^9 s^{-1} as an estimate for the maximum rate of collision of 1 M peptide chains at 20 °C and took this value to be the pre-exponential factor of the folding and unfolding direction.

The choice of the transmission coefficient κ of eq 4, the upper limit of which is 1, is more difficult. κ is an arbitrary constant to take into account repeated transitions through the folding barrier not explicitly included in conventional transition state theory. A κ of <1 means that the activation barrier is crossed many times before the transition ts → D occurs. That is, the activated state is sampled by diffusion as envisaged in Kramers' theory, which implicitly includes $\Delta S^{\ddagger}$ in the pre-exponential factor (*50*−*54*).

Indeed, it has been shown that folding of the GCN4 leucine zipper changes with the temperature-dependent solvent viscosity and that diffusion-limited chain movements can influence the rate-limiting step to folding, even though folding is much slower than the diffusion limit of encounter of the unfolded monomers (*55*). Hence, values of $\Delta S^{\ddagger}$ and $\Delta G^{\ddagger}$ not only do depend on the choice of the pre-exponential factor k_0 but also may be overestimated when using a κ of 1. Nevertheless, the changes in $\Delta S^{\ddagger}$ and $\Delta G^{\ddagger}$ with temperature can still be interpreted (see below and Figure 5).

Folding of the Leucine Zipper Domain of C62GCN4. In dimeric C62GCN4, a C-terminal leucine zipper domain joins two N-terminal basic regions, which bind to the major groove of the AP-1 or CRE site in a "scissors-grip" manner (*28*, *42*, *56*). The leucine zipper domain forms by association of the free peptides in the absence of DNA, but the N-terminal basic regions of dimeric C62GCN4 have no stable conformation when not bound to the target DNA, as shown by NMR spectroscopy (*41*). Thus, the dimeric coiled coil conformation does not continue into the basic region of C62GCN4, which lacks the repeating heptad pattern of the coiled coil. Therefore, the rate constants of folding deduced from the quenching of the C-terminal fluorescent label pertain only to the folding of the coiled coil domain. However, some partial helical structure may develop in the N-terminal segment at low temperatures. This is indicated by a very small shoulder in the CD melting curve at <30 °C (Figure 2A and ref *43*). However, this minor helical component does not substantially contribute to the thermodynamics of folding, which is clearly two-state (ref *34* and Figure 2B).[2]

$\Delta C_p^{\ddagger}$ and the Nature of the Transition State. The equilibrium thermodynamic parameter ΔC_p has been shown to correlate with the exclusion of nonpolar groups from the solvent. ΔC_p of protein folding is large and negative in the direction unfolded → folded (*58*−*61*). Therefore, the value of $\Delta C_p^{\ddagger}{}_{2M\rightarrow ts}$ should relate to the amount of nonpolar groups buried in the activated state of folding. One can define the ratio α_F ($=\Delta C_p^{\ddagger}{}_{2M\rightarrow ts}/\Delta C_p$) as a measure of the relative burial of hydrophobic surface area in the activated and folded states (*23*, *24*). An α_F close to 0 indicates a transition state near

[2] Folding of an α-helix contributes about 15 J K^{-1} (mol of residue)$^{-1}$ to ΔC_p (*57*). Therefore, if the basic region were 25% helical, this would contribute less than 10% to the overall ΔC_p of −2.8 kJ mol^{-1} K^{-1}. In fact, the helix content of the basic region was less than 25% in the refolding buffer, which contained 0.2 M GdmCl.

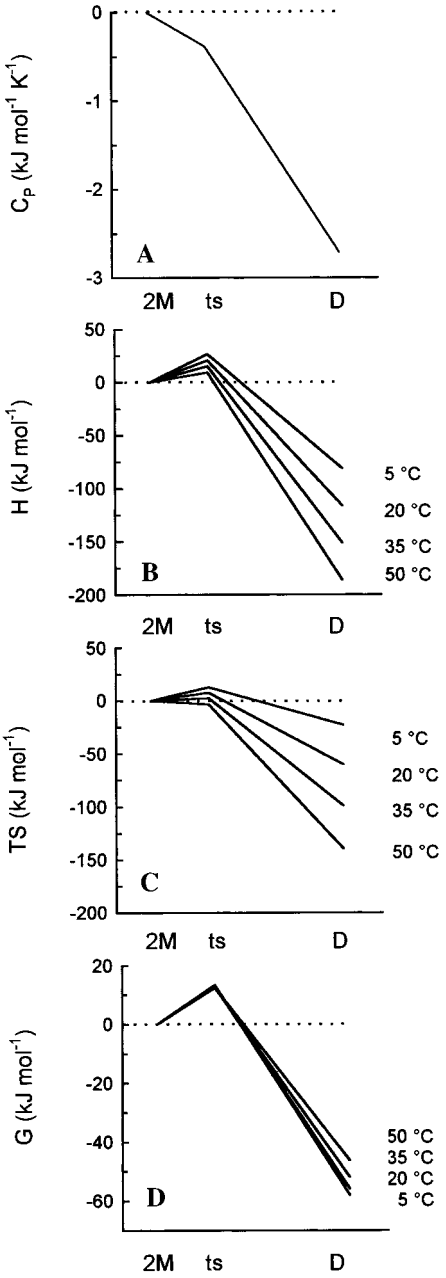

FIGURE 5: Reaction profile for the folding of the leucine zipper domain of yeast transcription factor GCN4. The abscissa shows that the reaction proceeds from two unfolded monomers M through the dimeric transition state ts to the folded dimer D. The changes in heat capacity (A), enthalpy (B), entropy (C), and free energy (D) are shown. Reference points are set arbitrarily at the monomeric state.

the unfolded state. An α_F close to 1 indicates a native-like transition state. The α_F of the leucine zipper domain of C62GCN4 is 0.1−0.2. Hence, the activated state is only 10−20% native-like in terms of buried nonpolar surface area. This is exceptional as the transition state of small single-domain proteins is usually closer to the folded than to the unfolded state when deduced from *m* values, which measure the change in folding free energy with denaturant concentration [$\alpha_F = m_{U\rightarrow ts}/m$ (*20*)]. For many small monomeric proteins, α_F values obtained from denaturant unfolding are in the range of 0.5−0.95 (*62*). There are only a few α_F values for dimeric proteins with which to compare our $\Delta C_p^{\ddagger}$-derived α_F values. The dimeric Arc and Trp repressors fold from unfolded monomers, and their transition states of folding,

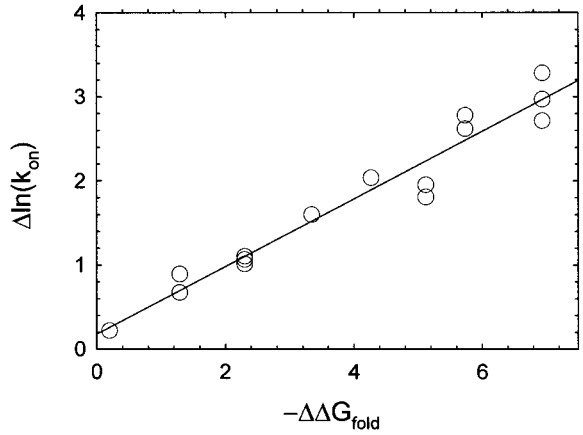

FIGURE 6: Increase of the folding rate of A_2 with coiled coil stability. The data were taken from Figures 4 and 9 of Dürr et al. (*12*). See the text for details on how $\Delta\ln(k_{on})$ and $\Delta\Delta G_{fold}$ were obtained. The solid line is a linear best fit with a slope α_F of 0.4, indicating that the activated state is 40% native.

deduced from *m* value analysis, are ∼70% native (*63*, *64*). Binding of the S-peptide to the folded S-protein of ribonuclease A reveals an activated state that is 66% native-like (*27*).

Since *m* values are thought to reflect the same phenomenon as ΔC_p values, α_F ratios deduced from $\Delta C_p^{\ddagger}$ and from *m* should be similar (*65*). For the GCN4 leucine zipper domain, α_F values deduced from denaturant unfolding as well as from the change of folding rates with denaturant concentration are between 0.4 and 0.6 (*13*, *21*, *22*, *55*), significantly different from the present α_F of 0.1−0.2. Φ value analysis[3] for a series of GCN4 mutants implies that the activated state of GCN4 leucine zipper folding is about 30% native-like (*22*), closer to our value from $\Delta C_p^{\ddagger}$. Still, the reason for the discrepant α_F values obtained by different experimental approaches is not clear. It has been noted by others that estimates of the placement of the activated state obtained from $\Delta C_p^{\ddagger}$ are systematically lower than those obtained from denaturant unfolding. For example, the transition state of folding of the dimeric Trp repressor is 76% native when estimated from *m* value analysis (*66*) and only 43% native when estimated from $\Delta C_p^{\ddagger}$ (*64*). The inconsistency was argued to originate from the fact that the burial of hydrophilic area does not contribute to *m* values, whereas it contributes negatively to ΔC_p (*64*). Several other instances of discrepant α_F values have been reported (*26*, *27*, *67*−*69*).

As mentioned above, the absolute values of $\Delta S^{\ddagger}$ and $\Delta G^{\ddagger}$ are overestimated if viscosity-dependent diffusive movements of the polypeptide contribute to the folding rate. This, however, would not change the qualitative relationship of the thermodynamic activation parameters of folding of C62GCN4 depicted schematically in Figure 5. $\Delta H^{\ddagger}_{2M\rightarrow ts}$ and $T\Delta S^{\ddagger}_{2M\rightarrow ts}$ change only slightly with temperature (panels B and C of Figure 5), and $\Delta G^{\ddagger}_{2M\rightarrow ts}$ is almost constant from 5 to 50 °C (panel D). The reason is that only 15% of the overall ΔC_p is achieved in the transition 2M → ts (panel A). In contrast, $\Delta H^{\ddagger}_{ts\rightarrow D}$ and $T\Delta S^{\ddagger}_{ts\rightarrow D}$ vary strongly with temperature in the transition ts → D where the bulk of the heat capacity change takes place. In other words, the overall

[3] Φ_F (equivalent to α_F) = $\Delta\Delta G_{2M\rightarrow ts}/\Delta\Delta G_{2M\rightarrow D}$, where ΔΔ refers to the difference between mutant and wild-type GCN4.

folding is enthalpically driven and opposed by a negative change of entropy, the main gain in enthalpy and the main loss in entropy being accomplished after the transition state. This is a clear indication of a not yet well structured transition state.

Folding of Coiled Coil A_2. Are the low structural content of the activated state and the major energetic changes taking place after the crossing of the transition state a peculiarity of the GCN4 leucine zipper? This does not seem to be the case since the folding of the unrelated dimeric coiled coil A_2 exhibits very similar features. Apart from the common heptad pattern, the two coiled coils are not sequence-related. Unlike the GCN4 zipper, A_2 exhibits no inter- or intrahelical electrostatic bonds and folding is purely "hydrophobic" and considerably faster than that of GCN4 (*12*). Nevertheless, the folding energetics of both zippers are quite similar. For both, the major energetic transitions occur in the step ts $\rightarrow$ D, and for both, the transition state is less structured than reported for monomeric single-domain proteins, 10−20% for the GCN4 zipper and 30−40% for A_2.

The major driving force of folding of A_2 is the protonation of the Glu side chains occupying the *e* and *g* positions of peptide A. This provides an independent way of deducing an α_F value from the change in the folding and unfolding rate with pH reported previously (*12*). When the pH is lowered, the folding rate constant k_{on} increases, and the dissociation rate decreases, resulting in an overall higher stability of A_2 at low pH (*12*). A large increase in k_{on} with decreasing pH means that removing the charges on the Glu side chains of A_2 stabilizes the activated state. A small increase indicates that the stabilizing effect of the protonation of Glu's is accomplished only after crossing through the activated state. Figure 6 shows the plot of $\Delta\ln(k_{on})$ versus $\Delta\Delta G_{fold}$ based on our previously published experiments. Rate and equilibrium constants were related to the values measured at pH 5.2, the midpoint of the pH−stability curve of A_2 (*12*). To obtain $\Delta\ln(k_{on})$ and $\Delta\Delta G_{fold}$, the pH 5.2 values of $\ln(k_{on})$ and ΔG_{fold}, respectively, were subtracted from the respective values measured between pH 5.2 and 4. The linear best fit to the data of Figure 5 yields a slope α_F of 0.4, in good agreement with an α_F of 0.3−0.4 from $\Delta C_p^{\ddagger}$.

General Conclusions about the Folding of Coiled Coils. From a large body of thermodynamic data, it is now clear that the strong increase with temperature of the enthalpy and entropy of folding originates mainly from large changes in the solvent−protein and solvent−solvent interaction, i.e., from the "hydrophobic effect". The unfavorable loss of conformational entropy of folding, which is weakly temperature-dependent, is opposed by the hydrophobic effect, which is strongly temperature-dependent (*23*, *24*). In coiled coil folding, these large changes seem to occur mostly *after* the transition state. This is the most striking conclusion of the study presented here since in most other cases the activated state resembles the folded state more than the unfolded state (recent reviews in refs *4* and *62*).

One possible explanation for the low α_F values of our two coiled coils could be that the activated state is in fact not a dimer but a partially folded monomer. It has been proposed that coiled coils fold by association of partially helical monomers. Therefore, one could argue that the activated state corresponds to an "association competent" monomer. We can rule out this possibility because of the design of our kinetic experiments; the measured rates reflect the change in fluorescence emission of peptides C62GCN4^{TR} and Flu-A, and the observed fluorescence decrease can only take place in the dimer (*44*, *45*). A pre-equilibrium between unfolded and partly helical monomers would be spectroscopically silent and would not contribute to the time-dependent fluorescence decrease. Hence, the activation parameters pertain to a dimeric transition state.

The question remains with respect to the amount of helical structure formed in the activated dimer, about which we can only speculate. On the one extreme is folding by a hydrophobic collapse mechanism with little or no helical structure present in the transition state (*13*). This model is difficult to relate to a modest amount of buried nonpolar surface area in the transition state. At the other extreme is the framework model of folding in which helices would form first and the rate-limiting step would be a rearrangement of an already helical dimer to the final parallel and in register coiled coil. This also is an unlikely model because of the low probability of helical monomers and of an all-helical transition state with the helices not yet juxtaposed as in the final coiled coil. A mechanism between a hydrophobic collapse and a framework model of folding follows from the observation of the main enthalpy gain occurring after the activated state and the buried nonpolar surface being not yet well developed in the activated state. This can be explained tentatively by an activated dimeric state with some helical structure yet very incomplete formation of tight helical interface, perhaps only where partial helices are already close to each other. Such an interpretation is in agreement with a folding mechanism in which partly helical domains of two peptide chains associate (*15*, *17*, *21*, *22*). Once a partly helical dimeric folding nucleus has been formed, folding to the final native dimer would be rapid. There could be a specific "trigger sequence" that has to be helical for the rate-limiting dimeric folding nucleus to develop (*15*). Alternatively, helical folding nuclei could develop at different places along the peptide chains (*21*). Determination of thermodynamic activation parameters for a set of mutants of the alleged helix trigger sequence might clarify this point.

ACKNOWLEDGMENT

We thank Dr. Stefan Klauser for peptide synthesis, Dr. Antonio Baici for allowing us to use his stopped-flow instrument and for valuable advice, and Dr. Thomas Kiefhaber for a preprint of ref *50*.

REFERENCES

1. Honig, B. (1999) *J. Mol. Biol. 293*, 283−293.
2. Baldwin, R. L. (1999) *Nat. Struct. Biol. 6*, 814−817.
3. Brockwell, D. J., Smith, D. A., and Radford, S. E. (2000) *Curr. Opin. Struct. Biol. 10*, 16−25.
4. Bilsel, O., and Matthews, C. R. (2000) *Adv. Protein Chem. 53*, 153−207.
5. Crick, F. H. C. (1953) *Acta Crystallogr. 6*, 689−697.
6. Cohen, C., and Parry, D. A. D. (1990) *Proteins 7*, 1−15.
7. Lupas, A. (1996) *Trends Biochem. Sci. 21*, 375−382.
8. Hope, I. A., and Struhl, K. (1987) *EMBO J. 6*, 2781−2784.
9. Landschulz, W. H., Johnson, P. F., and McKnight, S. L. (1988) *Science 240*, 1759−1764.
10. Hurst, H. C. (1996) *Leucine Zippers: Transcription factors*, 3rd ed., Academic Press, London.
11. Wendt, H., Leder, L., Härmä, H., Jelesarov, I., Baici, A., and Bosshard, H. R. (1997) *Biochemistry 36*, 204−213.

12. Dürr, E., Jelesarov, I., and Bosshard, H. R. (1999) *Biochemistry 38*, 870−880.
13. Sosnick, T. R., Jackson, S., Wilk, R. R., Englander, S. W., and Degrado, W. F. (1996) *Proteins 24*, 427−432.
14. Karplus, M., and Weaver, D. L. (1994) *Protein Sci. 3*, 650−668.
15. Kammerer, R. A., Schulthess, T., Landwehr, R., Lustig, A., Engel, J., Aebi, U., and Steinmetz, M. O. (1998) *Proc. Natl. Acad. Sci. U.S.A. 95*, 13419−13424.
16. Frank, S., Lustig, A., Schulthess, T., Engel, J., and Kammerer, R. A. (2000) *J. Biol. Chem. 275*, 11672−11677.
17. Myers, J. K., and Oas, T. G. (1999) *J. Mol. Biol. 289*, 205−209.
18. Fersht, A. R., Matouschek, A., and Serrano, L. (1992) *J. Mol. Biol. 224*, 771−782.
19. Fersht, A. R. (1995) *Curr. Opin. Struct. Biol. 5*, 79−84.
20. Fersht, A. R. (1999) *Structure and mechanism in protein science*, W. H. Freeman, New York.
21. Moran, L. B., Schneider, J. P., Kentsis, A., Reddy, G. A., and Sosnick, T. R. (1999) *Proc. Natl. Acad. Sci. U.S.A. 96*, 10699−10704.
22. Zitzewitz, J. A., Ibarra-Molero, B., Fishel, D. R., Terry, K. L., and Matthews, C. R. (2000) *J. Mol. Biol. 296*, 1105−1116.
23. Makhatadze, G. I., and Privalov, P. L. (1994) *Biophys. Chem. 51*, 291−309.
24. Makhatadze, G. I., and Privalov, P. L. (1995) *Adv. Protein Chem. 47*, 307−425.
25. Chen, B. L., and Schellman, J. A. (1989) *Biochemistry 28*, 685−691.
26. Schindler, T., and Schmid, F. X. (1996) *Biochemistry 35*, 16833−16842.
27. Goldberg, J. M., and Baldwin, R. L. (1998) *Biochemistry 37*, 2556−2563.
28. König, P., and Richmond, T. J. (1993) *J. Mol. Biol. 233*, 139−154.
29. Berger, C., Jelesarov, I., and Bosshard, H. R. (1996) *Biochemistry 35*, 14984−14991.
30. Berger, C., Piubelli, L., Haditsch, U., and Bosshard, H. R. (1998) *FEBS Lett. 425*, 14−18.
31. Gill, S. C., and von Hippel, P. (1989) *Anal. Biochem. 182*, 319−326.
32. Haughland, R. P. (1996) *Handbook of fluorescent probes and research chemicals*, 6th ed., Molecular Probes Inc., Leiden, The Netherlands.
33. Milla, M. E., and Sauer, R. T. (1994) *Biochemistry 33*, 1125−1133.
34. Thompson, K. S., Vinson, C. R., and Freire, E. (1993) *Biochemistry 32*, 5491−5496.
35. Zitzewitz, J. A., Bilsel, O., Luo, J. B., Jones, B. E., and Matthews, C. R. (1995) *Biochemistry 34*, 12812−12819.
36. Kentsis, A., and Sosnick, T. R. (1998) *Biochemistry 37*, 14613−14622.
37. Jelesarov, I., and Bosshard, H. R. (1996) *J. Mol. Biol. 263*, 344−358.
38. Jelesarov, I., Dürr, E., Thomas, R. M., and Bosshard, H. R. (1998) *Biochemistry 37*, 7539−7550.
39. Eyring, H. (1935) *J. Chem. Phys. 3*, 107−115.
40. Pappenberger, G., Saudan, C., Becker, M., Merbach, A. E., and Kiefhaber, T. (2000) *Proc. Natl. Acad. Sci. U.S.A. 97*, 17−22.
41. Bracken, C., Carr, P. A., Cavanagh, J., and Palmer, A. G. I. (1999) *J. Mol. Biol. 285*, 2133−2146.
42. Ellenberger, T. E., Brandl, C. J., Struhl, K., and Harrison, S. C. (1992) *Cell 71*, 1223−1237.
43. Weiss, M. A. (1990) *Biochemistry 29*, 8020−8024.
44. Wendt, H., Baici, A., and Bosshard, H. R. (1994) *J. Am. Chem. Soc. 116*, 6973−6974.
45. Wendt, H., Berger, C., Baici, A., Thomas, R. M., and Bosshard, H. R. (1995) *Biochemistry 34*, 4097−4107.
46. Berger, C. (1997) Ph.D. Thesis, pp 16−19, Faculty of Science, University of Zurich, Zurich.
47. Kohn, W. D., Kay, C. M., and Hodges, R. S. (1995) *Protein Sci. 4*, 237−250.
48. Hagen, S. J., Hofrichter, J., Szabo, A., and Eaton, W. A. (1996) *Proc. Natl. Acad. Sci. U.S.A. 93*, 11615−11617.
49. Bieri, O., Wirz, J., Hellrung, B., Schutkowski, M., Drewello, M., and Kiefhaber, T. (1999) *Proc. Natl. Acad. Sci. U.S.A. 96*, 9597−9601.
50. Bieri, O., and Kiefhaber, T. (2000) in *Mechanisms of protein folding: Frontiers in molecular biology* (Pain, R., Ed.) pp 34−64, Oxford University Press, Oxford, U.K.
51. Kramers, H. A. (1940) *Physica 4*, 284−304.
52. Jacob, M., Schindler, T., Balbach, J., and Schmid, F. X. (1997) *Proc. Natl. Acad. Sci. U.S.A. 94*, 5622−5627.
53. Klimov, V., and Thirumalai, D. (1997) *Phys. Rev. Lett. 79*, 317−320.
54. Jacob, M., Geeves, M., Holtermann, G., and Schmid, F. X. (1999) *Nat. Struct. Biol. 6*, 923−926.
55. Bhattacharyya, R. P., and Sosnick, T. R. (1999) *Biochemistry 38*, 2601−2609.
56. Vinson, C. R., Sigler, P. B., and McKnight, S. L. (1989) *Science 246*, 911−916.
57. Taylor, J. W., Greenfield, N. J., Wu, B., and Privalov, P. L. (1999) *J. Mol. Biol. 291*, 965−976.
58. Sturtevant, J. M. (1977) *Proc. Natl. Acad. Sci. U.S.A. 74*, 2236−2240.
59. Becktel, W. J., and Schellman, J. A. (1987) *Biopolymers 26*, 1859−1877.
60. Privalov, P. L., and Gill, S. J. (1988) *Adv. Protein Chem. 39*, 191−234.
61. Spolar, R. S., Livingstone, J. R., and Record, M. T., Jr. (1992) *Biochemistry 31*, 3947−3955.
62. Jackson, S. E. (1998) *Folding Des. 3*, R81−R91.
63. Waldburger, C. D., Jonsson, T., and Sauer, R. T. (1996) *Proc. Natl. Acad. Sci. U.S.A. 93*, 2629−2634.
64. Gloss, L. M., and Matthews, C. R. (1998) *Biochemistry 37*, 16000−16010.
65. Myers, J. K., Pace, C. N., and Scholtz, J. M. (1995) *Protein Sci. 4*, 2138−2148.
66. Gloss, L. M., and Matthews, C. R. (1998) *Biochemistry 37*, 15990−15999.
67. Tan, Y. J., Oliveberg, M., and Fersht, A. R. (1996) *J. Mol. Biol. 264*, 377−389.
68. Plaxco, K. W., Guijarro, J. I., Morton, C. J., Pitkeathly, M., Campbell, I. D., and Dobson, C. M. (1998) *Biochemistry 37*, 2529−2537.
69. van Nuland, N. A. J., Chiti, F., Taddei, N., Raugei, G., Ramponi, G., and Dobson, C. M. (1998) *J. Mol. Biol. 283*, 883−891.

BI002161L